Unique Structural and Transport Properties of Molybdenum Chalcohalide Nanowires

Igor Popov,[1] Teng Yang,[2] Savas Berber,[2] Gotthard Seifert,[1] and David Tománek[2]
[1]*Physikalische Chemie, Technische Universität Dresden, D-01062 Dresden, Germany*
[2]*Physics and Astronomy Department, Michigan State University, East Lansing, Michigan 48824-2320, USA*
(Received 21 February 2007; published 24 August 2007)

We combine *ab initio* density functional and quantum transport calculations based on the nonequilibrium Green's function formalism to compare structural, electronic, and transport properties of $Mo_6S_{6-x}I_x$ nanowires with carbon nanotubes. We find systems with $x = 2$ to be particularly stable and rigid, with their electronic structure and conductance close to that of metallic (13,13) single-wall carbon nanotubes. $Mo_6S_{6-x}I_x$ nanowires are conductive irrespective of their structure, more easily separable than carbon nanotubes, and capable of forming ideal contacts to Au leads through thio groups.

DOI: 10.1103/PhysRevLett.99.085503 PACS numbers: 81.05.Zx, 61.46.−w, 68.65.−k, 73.22.−f

Chalcohalides of molybdenum and other transition metals are known to form stable, intriguing two- and one-dimensional structures [1] with an unusual combination of electronic properties [2] including good conductance, superconductivity, magnetism, and nonlinear polarizability. These layered or filamentous substances are known as catalysts [3] and, to a much larger degree, as excellent solid lubricants [3–5]. Their potential to become unique building blocks of nanodevices has barely been noticed so far [3], in stark contrast to popular carbon nanotubes [6]. Recent progress in the synthesis of $Mo_xS_yI_z$ nanowires [7] suggests that these monodisperse, self-supporting nanostructures may nicely complement carbon nanotubes by avoiding their shortcomings such as a strong dependence of conductivity on the nanotube structure and difficulty to separate bundled tubes [6].

Here we combine *ab initio* density functional theory [8,9] and quantum transport calculations based on the nonequilibrium Green's function formalism [10,11] to compare structural, electronic, and transport properties of $Mo_6S_{6-x}I_x$ nanowires (NWs) to those of carbon nanotubes (CNTs). We find systems with $x = 2$ to be particularly stable and rigid, with their electronic structure and conductance close to that of metallic (13,13) single-wall carbon nanotubes. $Mo_6S_{6-x}I_x$ nanowires are conductive irrespective of their structure and capable of forming ideal contacts to Au leads through thio groups. Because of the weak interwire interaction, $Mo_6S_{6-x}I_x$ systems should be more easily separable than carbon nanotubes.

As mentioned before, chalcogenide compounds containing Mo and S have been studied for a long time [1,12]. Whereas the best known allotropes, including MoS_2, are insulating and form layered compounds, more interesting structures often occur at lower sulfur concentrations. Well known are Chevrel phases, characterized as cluster compounds with Mo_6S_8 subunits, furthermore finite clusters with a similar structure, and needlelike quasi-1D compounds [13]. All these interesting structures necessitate the presence of metal counterions for their synthesis. Besides providing structural stability, the main role of the counterions is to transfer electrons into the chalcogenide substructures [14,15], thereby forming an ionic crystal [16]. In their most stable electronic configuration, many of these compounds contained $(Mo_6S_6)^{2-}$ building blocks [12].

The idea behind this work is to study the possibility of stabilizing Mo-based nanowires by substituting the divalent sulfur by a monovalent halogen (I) with a similar electronegativity. In this way, the ''magic'' electronic configuration could be preserved, while maintaining a covalent character of the system and avoiding the formation of an ionic crystal, where electron correlations would dominate the electronic structure. In the following, we study the properties of $Mo_6S_{6-x}I_x$ nanowires, where iodine was used to substitute for sulfur.

To gain insight into structural and electronic properties of the proposed systems, we optimized the geometry of infinite $Mo_6S_{6-x}I_x$ nanowires for $x = 0$–6 using density functional theory (DFT). We used the Perdew-Zunger [17] form of the exchange-correlation functional in the local density approximation (LDA) to DFT, as implemented in the SIESTA code [18]. The behavior of valence electrons was described by norm-conserving Troullier-Martins pseudopotentials [19] with partial core corrections. We used a double-zeta basis, including initially unoccupied Mo5p orbitals.

Our numerical results were obtained for the primitive unit cell of length a, containing 12 atoms, depicted in Fig. 1(a). For selected structures, we also compared our results to those for a double unit cell with 24 atoms. To describe isolated nanowires while using periodic boundary conditions, we arranged them on a tetragonal lattice with a large interwire separation of 20 Å. We sampled the rather short Brillouin zone of these 1D structures by at least 8 k points. The charge density and potentials were determined on a real-space grid with a mesh cutoff energy of 150 Ry, which was sufficient to achieve a total energy convergence of better than 2 meV/atom during the self-consistency iterations.

To accelerate the global structure optimization of the nanowires with 36–72 degrees of freedom per unit cell, we first explored the configurational space and preoptimized

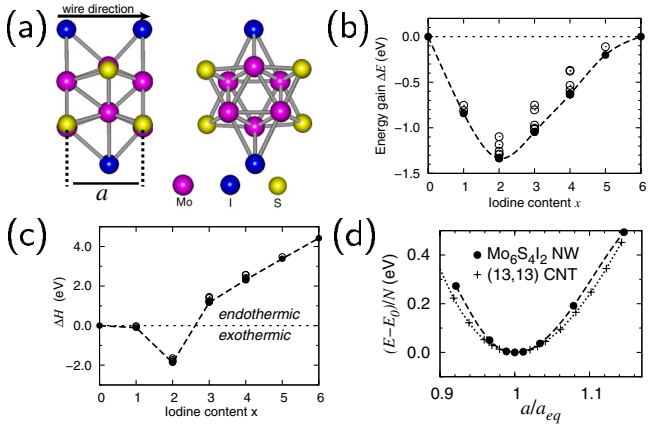

FIG. 1 (color online). (a) Schematic structure of a $Mo_6S_{6-x}I_x$ nanowire in side and end-on view. (b) Energy gain $\Delta E(x)$ with respect to the average binding energy [23] and (c) energy $\Delta H(x)$ of the substitution reaction in Eq. (1) leading to the formation of a $Mo_6S_{6-x}I_x$ nanowire as a function of composition. Among the data points for all structural isomers (○), the most stable structures are identified by the solid circles (•). (d) Deviation from the equilibrium binding energy E_0 as a function of the relative unit cell size a/a_{eq}, for a segment of the magic $Mo_6S_4I_2$ nanowire containing N Mo atoms, and for an N-atom segment of the (13,13) carbon nanotube.

the systems using the faster density functional based tight binding (DFTB) method [20,21], which had been used successfully to describe the deformation of MoS_2 layers to tubular structures [22].

The optimized structure of $Mo_6S_{6-x}I_x$ nanowires, shown in Fig. 1(a), consists of a Mo backbone decorated by S and I ligands. The Mo core structure is formed by Mo trimers of alternating orientation forming a chain. There is one Mo_6 octahedron per unit cell, surrounded by $(6-x)$ sulfur atoms and x iodine atoms. For each value of x we performed an exhaustive isomer search and a global structure optimization. In general, we find the Mo-Mo bond length to increase from ≈ 2.6 Å when close to sulfur, to ≈ 2.7 Å when close to the larger iodine. Introduction of iodine also causes an increase of the equilibrium lattice constant from $a_{eq}(Mo_6S_6) = 4.34$ Å to $a_{eq}(Mo_6I_6) = 4.55$ Å.

We find $Mo_6S_{6-x}I_x$ nanowires to be rather stable, with an average binding energy per atom ranging from 5.0 eV in Mo_6I_6 to 6.3 eV in Mo_6S_6 with respect to isolated atoms. The nanowires thus rival the stability of graphite with 7.3 eV/atom, and the slightly less stable carbon nanotubes. Changing the iodine content x in $Mo_6S_{6-x}I_x$ nanowires, we could naïvely expect the binding energy E to vary linearly between that of Mo_6S_6 and Mo_6I_6, showing no dependence on the particular structural isomer. In reality, deviations from this linear behavior [23], depicted as ΔE in Fig. 1(b), are substantial, suggesting that the stability of the various structural isomers at a particular composition varies by up to a large fraction of an eV. Focusing on the most stable isomers, we find a general tendency to selectively stabilize particular chalcohalide stoichiometries, such as $Mo_6S_4I_2$. As we will show below, this magic composition optimizes the electronic configuration of the building blocks to agree with the optimum charge state identified above using heuristic arguments.

Among the many structural isomers of $Mo_6S_{6-x}I_x$, we generally found structures with the largest separation between iodine atoms to be most stable. When increasing the variational freedom in the arrangement of iodine atoms by doubling the unit cell size, we identified geometries that further stabilize the structures by providing energy gain per unit cell ranging from 0.09 eV for $x = 1$ to 0.29 eV for $x = 3$.

The selectivity of a possible synthesis pathway becomes apparent, when studying the reaction energy ΔH of the substitution reaction

$$Mo_6S_6 + \frac{x}{2}I_2 \xrightarrow{\Delta H} Mo_6S_{6-x}I_x + \frac{x}{8}S_8, \qquad (1)$$

depicted in Fig. 1(c). Clearly, substitution of sulfur in Mo_6S_6 by gas-phase iodine is only exothermic for the magic iodine content $x = 2$.

In the following, we will compare various properties of $Mo_6S_{6-x}I_x$ nanowires to those of carbon nanotubes. As will become clear later on, the electronic structure of the chalcohalide nanowires matches well that of a conducting (13,13) carbon nanotube with a diameter of 17.6 Å. The equilibrium unit cell size $a_{eq}(13, 13) = 2.46$ Å of the armchair nanotube is about half the value of the magic nanowire, $a_{eq}(Mo_6S_4I_2) = 4.45$ Å.

The axial stiffness of a $Mo_6S_4I_2$ nanowire in comparison to that of a (13,13) carbon nanotube can be inferred from Fig. 1(d). We feel that in a fair comparison between the different systems, the energy investment upon axial strain should be normalized by the number of Mo backbone atoms in the nanowire and number of C atoms in the nanotube. Inspection of our results in Fig. 1(d) suggests that the high axial stiffness, based on the above definition, is nearly the same in the two systems. Thus, the $Mo_6S_4I_2$ nanowire differs significantly in its rigidity from the accordionlike behavior identified recently in the "floppy" $Mo_6S_{4.5}I_{4.5}$ nanowire [24].

Contrasting with the high stability and axial stiffness of the $Mo_6S_4I_2$ nanowires is their lateral interwire interaction, discussed in Fig. 2. We calculated the binding energy of straight nanowires on a simple hexagonal lattice with respect to isolated nanowires using DFTB, augmented by van der Waals interactions [25]. Our results for the binding energy as a function of the interwire separation d and the wire orientation φ are presented in Fig. 2(b). We find the binding energy to be generally weak and strongly anisotropic. The most stable arrangement occurs at an interwire separation $d = 9.3$ Å. The binding energy in this geometry corresponds to 0.1 eV for a 1 Å long nanowire segment and equals that of a corresponding segment of bundled (10,10) CNTs [26]. In realistic bundles, individual nanowires and nanotubes are likely to be twisted rather than being per-

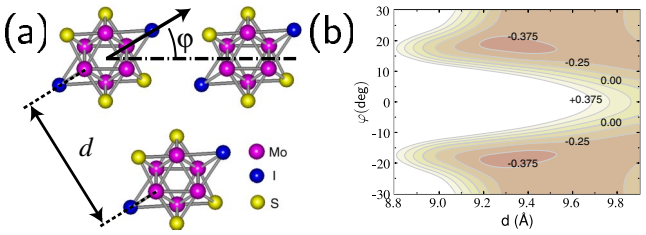

FIG. 2 (color online). (a) Structure of $Mo_6S_4I_2$ nanowires arranged on a simple hexagonal lattice in a plane normal to the wire axes. (b) Contour plot of the nanowire binding energy in this lattice as a function of the wire orientation φ and separation d. The energy is given in eV per formula unit.

fectly straight over long distances [27]. Then, their effective interaction should be closer to an average over all possible orientations. Because of its anisotropy, seen in Fig. 2(b), the effective attraction between $Mo_6S_4I_2$ nanowires is strongly reduced or changes to repulsion when averaging over φ, whereas the rather isotropic interaction between nanotubes does not affect their strong binding [26]. This explains the observation that bundled chalcohalide nanowires are much easier to separate than bundled carbon nanotubes.

Among the different properties of $Mo_6S_{6-x}I_x$ nanowires, we find their electronic structure to be most intriguing. In Fig. 3 we compare the band structure $E(k)$, the density of states (DOS), and ballistic conductance of isolated $Mo_6S_{6-x}I_x$ nanowires to those of an isolated (n, n) single-wall carbon nanotube. Independent of composition, we find all $Mo_6S_{6-x}I_x$ nanowires to be metallic or semimetallic. This is appealing in view of the fact that carbon nanotubes may be conducting or semiconducting, depending on their chiral index (n, m) [6].

In Figs. 3(a)–3(f), the electronic properties of the $Mo_6S_4I_2$ and the Mo_6S_6 nanowires can be compared side by side. External gating or doping can furthermore be used to shift the Fermi level of the chalcohalide NWs, as indicated by the dotted lines in Fig. 3. Similar to conducting (n, n) carbon nanotubes, we find an energy range with a constant DOS also near the Fermi energy of the gated chalcohalide NWs, suggesting high electron mobility, which is flanked by a pair of van Hove singularities. As can be seen by comparing Figs. 3(e) and 3(h), the energy separation of the van Hove singularities in the Mo_6S_6 nanowire is best matched by the metallic (13,13) carbon nanotube, which we consider here. For the sake of easy comparison with carbon nanotubes, we will focus on externally gated or doped chalcohalide NWs in the following.

The band dispersion of gated $Mo_6S_{6-x}I_x$ nanowires and the (13,13) carbon nanotube are compared in the left panels of Fig. 3. In all three systems considered we can identify nearly free-electron bands in the vicinity of E_F. Whereas the constant DOS near E_F in the (13,13) carbon nanotube, shown in Fig. 3(h), derives from bands of $C2p\pi$ character, a very similar constant DOS of Mo_6S_6 in Fig. 3(e) derives

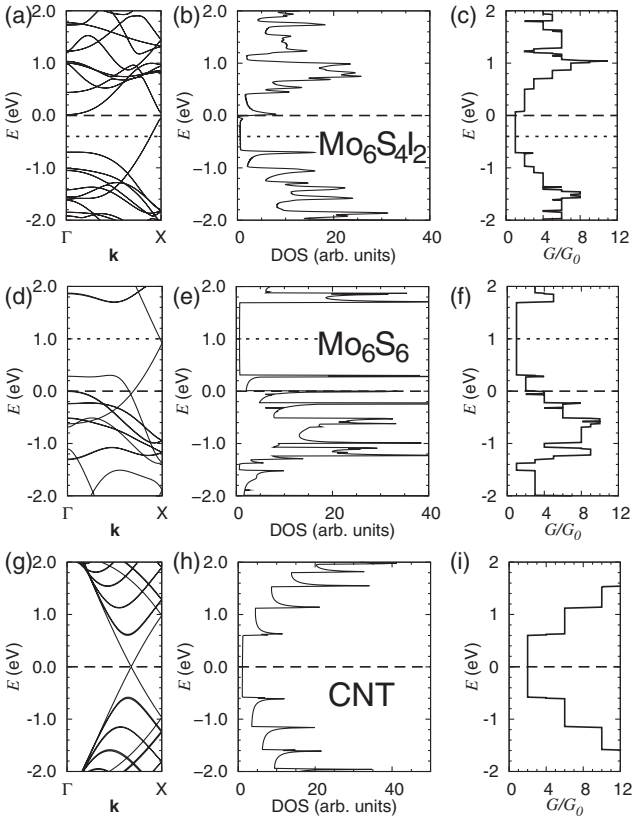

FIG. 3. Electronic properties of a $Mo_6S_{6-x}I_x$ nanowire (a)–(f) in comparison to a (13,13) carbon nanotube (g)–(i). Displayed is the band structure $E(k)$ of the $Mo_6S_{6-x}I_x$ nanowires in (a),(d), their DOS in (b),(e), and quantum conductance $G(E)$ in units of the conductance quantum G_0 (c),(f). The corresponding quantities for the (13,13) carbon nanotube are shown in (g)–(i). $E = 0$, given by the dashed lines, corresponds to the Fermi level in (a),(b),(d),(e),(g),(h), and to zero source-drain voltage in (c),(f),(i). The dotted lines show the position of E_F in externally gated or doped chalcohalide nanowires resembling carbon nanotubes.

from a_2 bands [12] with predominant Mo4$d\sigma$ character. In general, we expect the stability of any system to increase when populating bonding or depopulating antibonding states. In $Mo_6S_{6-x}I_x$ nanowires, the optimum stabilization is achieved by filling the Mo4d-derived a_2 band up to the folding point at X.

As suggested by comparing Figs. 3(a), 3(b), 3(d), and 3(e), we find that the main effect of changing the composition of $Mo_6S_{6-x}I_x$ nanowires by iodine substitution prior to gating is to electronically dope the system by shifting the Fermi level. This finding agrees qualitatively with that in $Li_xMo_6S_6$ nanowires [16], where the most stable $x = 2$ composition has been associated with the magic $(Mo_6S_6)^{2-}$ complexes. As suggested above, stabilization of the system should depend on the oxidation state of the Mo backbone. In that case, initial withdrawal of 12 electrons from Mo_6 by divalent sulfur ligands, followed by adding two electrons to Mo_6 in the magic $(Mo_6S_6)^{2-}$

complexes, should be equivalent to withdrawing only 10 electrons from Mo_6 in the first place, by substituting two divalent sulfurs by monovalent iodines. Further increase in the concentration of Li or I should increase the population of the antibonding levels and thus destabilize the system. We find this reasoning confirmed by the observed unusual stability of $Li_2Mo_6S_6$ and $Mo_6S_4I_2$, both of which should display a similar electronic configuration of the Mo backbone.

As seen in Figs. 3(a) and 3(d), substituting sulfur by iodine atoms in $Mo_6S_4I_2$ not only shifts the Fermi level, but also opens a narrow band gap, while introducing a new band above E_F. This nearly free-electron band of predominantly Mo4*d* character is also observed in the Li doped Mo_6S_6 system [16] and caused by locally changing the crystal potential along the chains of I or Li atoms in the crystal. We find the position of this band to depend sensitively on the lattice constant, suggesting the possibility to modify the electronic structure by axial deformation.

Addressing the usefulness of $Mo_6S_{6-x}I_x$ nanowires as ballistic conductors, we calculated their quantum conductance G as a function of the carrier injection energy E using the nonequilibrium Green's function approach [10,11]. The conductance results for $x = 2$ and $x = 0$, presented in Figs. 3(c) and 3(f), are compared to those for a (13,13) carbon nanotube in Fig. 3(i). In the gated chalcohalide NWs, the Mo4*d* character of the states near E_F suggests that conduction involves mostly the Mo backbone and not the ligands.

Since all these systems are metallic, with a constant density of states near E_F, we observe similarities in the conductance spectra of gated $Mo_6S_{6-x}I_x$ nanowires and metallic carbon nanotubes. A major advantage of $Mo_6S_{6-x}I_x$ nanowires is the natural termination of finite segments by sulfur atoms, which are known to bind to Au electrodes as thio groups in a well-defined way.

In conclusion, we combined *ab initio* density functional and quantum transport calculations to compare structural, electronic, and transport properties of $Mo_6S_{6-x}I_x$ nanowires with carbon nanotubes. We find that the $Mo_6S_4I_2$ system may form particularly stable, freestanding quasi-1D nanowires with electronic structure and conductance close to that of metallic (13, 13) single-wall carbon nanotubes. $Mo_6S_{6-x}I_x$ nanowires have advantageous properties in comparison to carbon nanotubes by being conductive irrespective of their structure, more easily separable, and capable of forming ideal contacts to Au leads through thio groups.

D. T. was supported by NSF NSEC Grant No. 425826, NSF NIRT Grant No. ECS-0506309, and the Humboldt Foundation.

[1] A. Simon, Angew. Chem., Int. Ed. Engl. **27**, 159 (1988).
[2] B. Bercic, U. Pirnat, P. Kusar, D. Dvorsek, D. Mihailovic, D. Vengust, and B. Podobnik, Appl. Phys. Lett. **88**, 173103 (2006).
[3] J. V. Lauritsen, J. Kibsgaard, S. Helveg, H. Topsøe, B. S. Clausen, E. Lægsgaard, and F. Besenbacher, Nature Nanotechnology **2**, 53 (2007).
[4] L. Rapoport, Y. Bilik, Y. Feldman, M. Homyonfer, S. R. Cohen, and R. Tenne, Nature (London) **387**, 791 (1997).
[5] L. Joly-Pottuz, F. Dassenoy, M. Belin, B. Vacher, J. Martin, and N. Fleischer, Tribol. Lett. **18**, 477 (2005).
[6] M. S. Dresselhaus, G. Dresselhaus, and P. Avouris, *Carbon Nanotubes: Synthesis, Structure, Properties and Applications* (Springer, Berlin, 2001).
[7] D. Vrbanic, *et al.*, Nanotechnology **15**, 635 (2004).
[8] P. Hohenberg and W. Kohn, Phys. Rev. **136**, B864 (1964).
[9] W. Kohn and L. Sham, Phys. Rev. **140**, A1133 (1965).
[10] J. Taylor, H. Guo, and J. Wang, Phys. Rev. B **63**, 245407 (2001).
[11] M. Brandbyge, J.-L. Mozos, P. Ordejón, J. Taylor, and K. Stokbro, Phys. Rev. B **65**, 165401 (2002).
[12] T. Hughbanks and R. Hoffmann, J. Am. Chem. Soc. **105**, 1150 (1983).
[13] M. Potel, R. Chevrel, M. Sergent, J. Armici, M. Decroux, and O. Fischer, J. Solid State Chem. **35**, 286 (1980).
[14] F. J. Ribeiro, D. J. Roundy, and M. L. Cohen, Phys. Rev. B **65**, 153401 (2002).
[15] L. Venkataraman and C. M. Lieber, Phys. Rev. Lett. **83**, 5334 (1999).
[16] S. Gemming, G. Seifert, and I. Vilfan, Phys. Status Solidi B **243**, 3320 (2006).
[17] J. P. Perdew and A. Zunger, Phys. Rev. B **23**, 5048 (1981).
[18] J. M. Soler, E. Artacho, J. D. Gale, A. García, J. Junquera, P. Ordejón, and D. Sánchez-Portal, J. Phys. Condens. Matter **14**, 2745 (2002).
[19] N. Troullier and J. L. Martins, Phys. Rev. B **43**, 1993 (1991).
[20] D. Porezag, T. Frauenheim, T. Köhler, G. Seifert, and R. Kaschner, Phys. Rev. B **51**, 12 947 (1995).
[21] G. Seifert, D. Porezag, and T. Frauenheim, Int. J. Quantum Chem. **58**, 185 (1996).
[22] G. Seifert, H. Terrones, M. Terrones, G. Jungnickel, and T. Frauenheim, Phys. Rev. Lett. **85**, 146 (2000).
[23] In analogy to the mixing energy, we define ΔE as the energy gain upon forming a $Mo_6S_{6-x}I_x$ nanowire from noninteracting Mo_6S_6 and Mo_6I_6 segments of proper length ratio.
[24] T. Yang, S. Okano, S. Berber, and D. Tománek, Phys. Rev. Lett. **96**, 125502 (2006).
[25] L. Zhechkov, T. Heine, S. Patchkovskii, G. Seifert, and H. Duarte, J. Chem. Theory Comput. **1**, 841 (2005).
[26] Y.-K. Kwon, D. Tománek, Y. H. Lee, K. H. Lee, and S. Saito, J. Mater. Res. **13**, 2363 (1998).
[27] Y.-K. Kwon and D. Tománek, Phys. Rev. Lett. **84**, 1483 (2000).